Spins of proton capture resonances in ^{26}Al and ^{30}P from their gamma-ray spectra

J. A. Cameron
Department of Physics and Astronomy, McMaster University, Hamilton, Ontario, Canada L8S 4K1
(Received 4 November 1992)

The method of multidimensional scaling has been applied to sets of proton capture γ-ray spectra in ^{26}Al and ^{30}P, allowing the attribution of spins to a number of resonances in each nucleus. The utility of this method of simultaneous comparison of many resonance decay branching patterns appears to depend on the variety of final state spins. In the case of ^{26}Al, where the spin discrimination is good, some selectivity by parity and isospin also occurs.

PACS number(s): 25.40.Lw, 25.40.Cm, 24.30.Gd, 27.30.+t

I. INTRODUCTION

Proton resonance spectroscopy provides a means to observe closely spaced nuclear levels at high excitation energy. With the exception of a relatively small number of levels of strong single-particle character such as analog states, most high-lying levels are of a highly complex nature, and the overall structure is best described using statistical measures [1]. It has been suggested that the variations in level density may be attributable to chaotic behavior in the small quantum system of the nucleus [2]. In order to compare the level system with such models, maximal information about the individual levels is still desirable. This includes not only their energies, but also their widths in all channels, and their spins, parities, and isospins—a complete spectroscopy.

Spins of proton resonances are usually derived from the angular distributions of elastically and inelastically scattered protons and of γ rays following inelastic scattering and capture. The former are generally reliable indicators of spin and parity for orbital angular momenta in the entrance channel $l \leq 2$ [1,3,4]. Capture γ-ray angular distributions are often of help at higher spin, where the elastic and inelastic cross sections may be small [5]. In all γ-ray angular distributions, the number of parameters which may be determined is limited by the low angular momentum of the radiation, and so ambiguities involving spins and multipole mixing ratios may arise. In establishing a unique spin assignment from capture data, it is usually necessary to eliminate ambiguities by observing transitions to two or more final states. Because capture cross sections are generally small, obtaining good angular distribution data often involves very long measurement times.

Under favorable circumstances, spins may be deduced reliably from the spectra alone. This follows from the selection rules for γ decay, which favor the low multipoles $E1$, $M1$, and $E2$. So, for example, a resonance which is seen to decay strongly to final states of $J^\pi = 0^+$ and 3^+ may be concluded to have spin-parity 1^+ or 2^+. If a further branch to a 3^- state is found, then the 1^+ choice becomes unlikely, leaving only 2^+. Such happy circumstances are, however, uncommon. Often, the spread of final state spins is not so great, and sometimes the states fed have uncertain spins.

An alternative approach is to consider the high degree of selection brought about by a very large number of soft constraints. Gamma transition rates, and their consequent branching ratios, belong to this class. Proton capture resonances are characterized by their high excitation energies and usually large number of decay branches. It is possible, in cases where considerable feeding and decay information is available, to use relative transition rates to make reliable spin inferences for individual states. A good example of such work, relevant to the present study, is that on ^{26}Al by Endt *et al.* [6].

An even more general method using decay branching only, and not requiring any knowledge of final state spins, starts from the premise that resonances of the same spin are likely to decay to the same subset of final states. A measure of similarity between two resonances may be found in the correlation between their spectra. In practice, branching amplitudes have been used [7]. These are written for each resonance as a unit vector in the space of final states. The scalar product of two such vectors measures the similarity.

The collection of entities, in this case proton resonances, into clusters from the analysis of the matrix of similarities between all pairs is the subject of a set of techniques known collectively as multidimensional scaling (MDS) [8,9]. It is an appealing advantage of the technique that no knowledge of spins of final states is required. Only spins of a number of representative resonances are required to form a "calibration" of the clustering. An initial demonstration of MDS to the analysis of capture spectra [7] indicated that the method had good success in an f-shell nucleus ^{59}Cu and less success in ^{19}F. Further tests were made recently in ^{49}V [10], ^{51,53}Mn, and ^{55}Co [11]. Here, to examine the qualities of the level schemes that are required for MDS to be useful in making spin determinations and to make a small contribution to the set of known resonance spins in two *sd* nuclei, the capture resonances of ^{26}Al and ^{30}P are studied.

The data are largely from the work of others. For ^{26}Al the spectra of Endt, De Wit, and Alderliesten [12] were used, while for ^{30}P results of Reinecke *et al.* [13] and Frankle *et al.* [14] were combined with the present measurements.

II. ^{30}P EXPERIMENT

The reaction ^{29}Si$(p,\gamma)^{30}$P was studied both at the King Saud University AK and McMaster University KN Van de Graaff accelerators, using methods described in earlier publications [4,10]. With the 8-μg/cm^2 targets used, the overall resolution was about 1 keV. A yield curve was measured from 2.0 to 3.0 MeV in proton beam energy, al-

TABLE I. Fifty resonances in ^{30}P.

No.	E_p (MeV)	E_x (MeV)	$J^\pi;T$
1	0.324	5.908	2^-
2	0.417	5.997	1
3	0.699	6.270	2^-
4	0.729	6.299	$3^+;0$
5	0.918	6.481	$1^+;0$
6	0.957	6.519	$1^+,2^+$
7	1.111	6.668	$2^-,3^+$
8	1.303	6.853	$1^+;0$
9	1.325	6.875	3^+
10	1.327	6.877	2^-
11	1.373	6.921	$1^-;0$
12	1.471	7.016	$2^-;0$
13	1.503	7.046	$2^-,3^-$
14	1.506	7.050	$4^-;1$
15	1.638	7.177	1^-
16	1.664	7.203	$1^+,2^+;0$
17	1.669	7.208	$1^+;1$
18	1.686	7.224	$2^-;1$
19	1.746	7.282	3
20	1.748	7.284	$2^+;1$
21	1.771	7.306	$2^-;0$
22	1.772	7.307	$2^-;0$
23	1.853	7.385	$1\text{-}4^+;0$
24	1.967	7.495	$1^+;0$
25	2.038	7.564	$2^+;1$
26	2.055	7.581	2^-
27	2.081	7.606	$3^+;0$
28	2.114	7.637	$2^-,3;1$
29	2.122	7.645	$3^+;1$
30	2.170	7.691	$3^+;0$
31	2.232	7.751	$1^+;0$
32	2.241	7.760	2;1
33	2.310	7.835	$2^-,3^-$
34	2.369	7.883	
35	2.406	7.927	2^+
36	2.408	7.928	
37	2.409	7.931	
38	2.490	8.008	1^-
39	2.498	8.011	$1\text{-}3^+$
40	2.506	8.019	2^+
41	2.522	8.027	$1^-,2^-$
42	2.599	8.117	2^+
43	2.660	8.165	1^-
44	2.683	8.198	3^-
45	2.702	8.206	4^-
46	2.706	8.209	0^-
47	2.777	8.279	2^+
48	2.889	8.397	3^+
49	2.936	8.432	2^+
50	3.033	8.527	

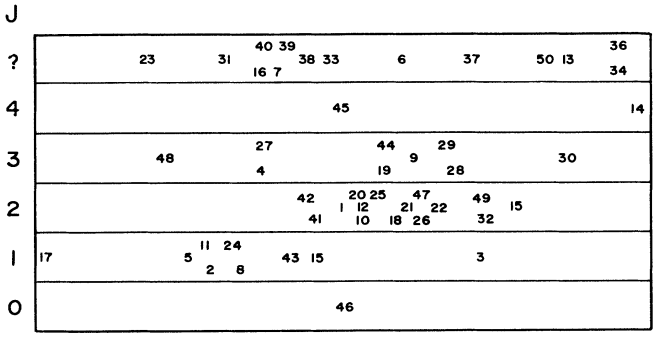

FIG. 1. One-dimensional MDS map of the ^{30}P resonances. The horizontal positions of the numbers representing the resonances are arranged so the separations best satisfy the conditions (1). The points are displaced vertically according to their spins J.

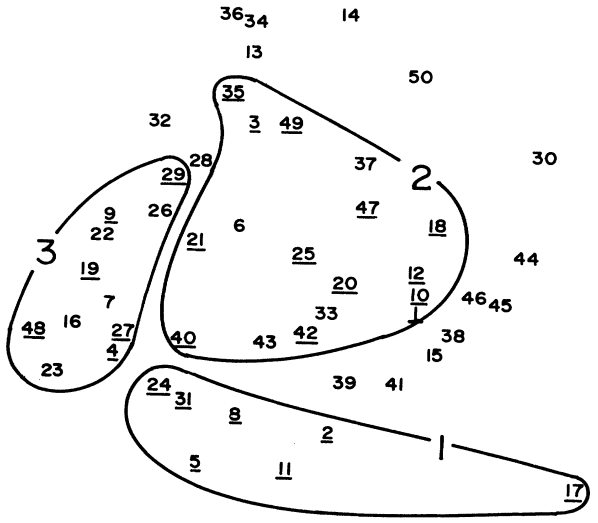

FIG. 2. Two-dimensional MDS map of the ^{30}P resonances. The conditions (1) are rotation, reflection, and scale invariant, and so the axes have no absolute meaning. The solid lines outline regions which may be assigned to a single spin.

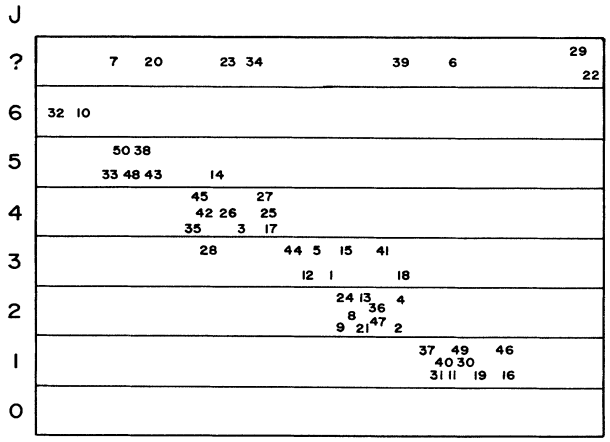

FIG. 3. One-dimensional MDS map of the ^{26}Al resonances, as in Fig. 1.

TABLE II. Decay of 14 resonances in ^{30}P observed in this work.

	Resonance no.																	
E_f (MeV)	33	34	35	36	37	38	39	40	41	42	43	44	45	46	47	48	49	50
0.0	67				32	75	57	9	20	75	28	26	51	88	25		8	4
0.677					3	32	2											
0.709	21		16		7			1	15						38		6	
1.455	7		9					3										
1.974		15	22	11	12										10		30	31
2.539		17	15	20	16										7		27	
2.724															6	6	9	
2.840		39		51	20												16	
2.938	5						7	64		25	31					32		
3.019						11	4				20		13		3			
3.734						8									3		2	
3.836			7		2						17				5			
3.929			13		3										3		2	
4.144											4	41	14					
4.183	21							21	32							33		
4.233												33	22	12				
4.298		5		3														8
4.344		24		15	5													38
4.627			9		1													
4.736			9		2													
5.207																		15
5.232																		4
5.509						3												
5.520									33							19		
6.010																10		

lowing some overlap with the results of Reinecke *et al.* [13], who measured in the range 0.3–2.3 MeV. The yield curve agrees well with the higher-resolution work of Frankle *et al.* [14]. Below 2.3 MeV, several spectra examined in Ref. [13] were observed and good agreement was found. In the region above 2.3 MeV, spectra were collected at the 18 resonances listed as 33–50 in Table I. The branching ratios for these resonances are given in Table II.

III. MDS ANALYSIS

The set of 50 resonances in Table I used for the study of ^{30}P was taken from the results above and from those of Reinecke *et al.* [13]. The spin, parity, and isospin values are from Refs. [13–15]. For 1–32, the branching data can be found in Table 2 of Ref. [13]. From the decay branching intensities I_{ik} for each resonance i to final states k, a unit vector $a_{ik}=I_{ik}^{1/2}$ was formed. The 50×50 triangular similarity matrix was constructed as suggested in Sec. I above and in Ref. [7] from the scalar products,

$$C_{ij}=\sum_k a_{ik}a_{jk} ,$$

and used as input to the program MINISSA [16], which produces a geometric model (map) in which the resonances are represented by points whose separation is a monotonely decreasing function of the similarities. That is,

$$\text{if } C_{ij}>C_{mn} , \quad \text{then } d_{ij}<d_{mn} , \tag{1}$$

where d_{ij} is the distance separating points representing resonances i and j. Figures 1 and 2 are the one- and two-dimensional maps which result. The numbers of the resonances are at the points. In Fig. 1 the data are dis-

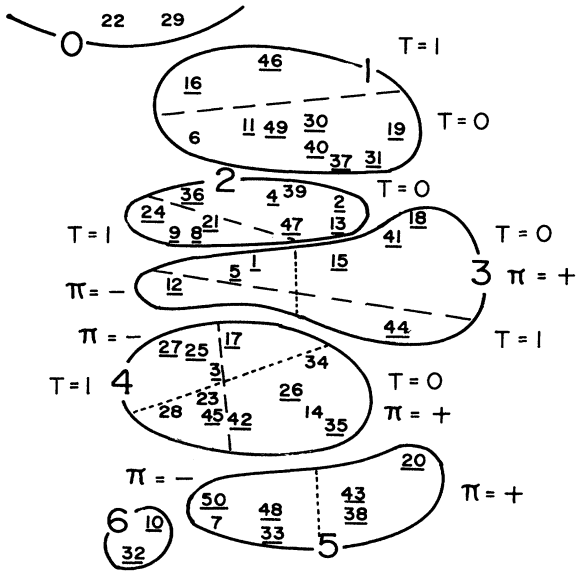

FIG. 4. Two-dimensional MDS map of the ^{26}Al resonances, as in Fig. 2. Within the solid boundaries of regions of a single spin, the dashed lines separate resonances of isospin, $T0$, and 1, and the dotted lines separate those of even and odd parity, π.

placed vertically to separate resonances of different spins, while the horizontal scale maps the similarities. Because conditions (1) are on separations, not positions, the resulting map is reflection invariant. Since they are inequalities, the scale in Fig. 1 is arbitrary. In Fig. 2 the enclosing lines suggest regions within which it seems reasonable to assume all resonances have the same spin, as labeled, with underlined resonances having known spins. Again, the conditions (1) allow invariance of the map under reflection, rotation, and scale changes.

As a second example of the technique, the results of Endt *et al.* [6,12] for resonances in the reaction ^{25}Mg$(p,\gamma)^{26}$Al were treated in the same way. A set of 50 resonances, including all of those for which spectra were available but no unique spin determination had been made, as well as a well-distributed set of "calibrating" resonances of known spin, was chosen (Table III). The corresponding one- and two-dimensional MDS maps are shown in Figs. 3 and 4. In this case the spin discrimination is much clearer in both one and two dimensions.

TABLE III. Fifty resonances in ^{26}Al.

No.	E_p (MeV)	E_x (MeV)	$J^\pi;T$
1	0.317	6.610	$3^-;0$
2	0.390	6.680	$2^+;0$
3	0.435	6.724	$4^-;0$
4	0.497	6.784	$2^-;0$
5	0.503	6.787	$3^-;0$
6	0.516	6.802	$1,2^-;0$
7	0.530	6.816	$4,5,6^+;0$
8	0.567	6.852	2^+
9	0.593	6.876	$2^+;1$
10	0.609	6.892	$6^-;0$
11	0.656	6.936	$1^+;0$
12	0.685	6.964	$3^-;1$
13	0.723	7.001	$2^+;0$
14	0.738	7.015	$5^+;0$
15	0.775	7.051	$3^+;0$
16	0.811	7.086	$1^-;1$
17	0.835	7.109	$4^-;0$
18	0.881	7.153	$3^+;0$
19	0.928	7.198	$1^+;0$
20	0.953	7.222	$5^+;1$
21	0.986	7.254	$2^-;1$
22	1.019	7.286	0^--2;0
23	1.025	7.292	$3^+,4^+;0$
24	1.043	7.308	$2^+;1$
25	1.084	7.348	$4^-;1$
26	1.103	7.366	$4^+;0$
27	1.148	7.410	$4^-;1$
28	1.164	7.425	$3^+;0$
29	1.179	7.440	0-2;1
30	1.184	7.444	$1^-;0$
31	1.196	7.455	$1^+;0$
32	1.273	7.529	$6^-;0$
33	1.292	7.548	$5^-;0$
34	1.337	7.592	$3^+,4^+;0$
35	1.342	7.596	$4^+;0$
36	1.351	7.605	$2^-;0$
37	1.370	7.623	$1^+;0$
38	1.375	7.628	$5^+;1$
39	1.396	7.648	$1^+,2^+;0$
40	1.568	7.814	$1^+;0$
41	1.632	7.874	$3^+;0$
42	1.649	7.891	$4^+;0$
43	1.680	7.921	$5^+;0$
44	1.699	7.939	$3^+;1$
45	1.714	7.953	$4^+;1$
46	1.763	8.001	$1^-;1$
47	1.771	8.008	$2^+;0$
48	1.774	8.011	$5^-;1$
49	1.800	8.036	$1^-;0$
50	1.832	8.067	$5^-;1$

TABLE IV. New resonance spins in ^{26}Al.

Resonance no.	E_p (MeV)	$J^\pi;T$ a	b
6	0.516	$1,2^-;0$	1;0
7	0.530	$6^+(4,5);0$	5^-
14	0.738	$5^+;0$	$4^+;0$
22	1.019	$0^-(1,2);0$	0
23	1.025	$4^+(3^+);0$	4
28	1.164	$3^+;0$	4;1
29	1.179	0(1,2);1	0
34	1.337	$4^+(3^+);0$	$4^+;0$
39	1.396	$1^+(2^+);0$	$2^+;0$

[a]Reference [15].
[b]MDS, Fig. 4.

IV. DISCUSSION

The new spins attributable to the resonances of ^{26}Al and ^{30}P on the basis of their decay choices to states of known spin and on that of the MDS analyses of decay branching patterns are shown in Tables IV and V, respectively. In ^{26}Al, the analysis of Refs. [6] and [16] coincide. In all cases but two, resonances 14 and 28, the MDS analysis yields spins consistent with those given by Refs. [6,16]. In two cases, resonances 7 and 39, a spin less favored is selected.

In ^{30}P, for which the spin discrimination of the MDS method is less clear than in ^{26}Al, unique spin attributions are only possible for 6 of the 13 resonances previously unassigned. Of the remainder, however, most are more restrictively defined by the MDS analysis than by separate consideration of the decay schemes. Only for resonance 37 does the MDS analysis yield a spin inconsistent with that from the decay scheme.

It is evident from a comparison of Figs. 1 with 3 and 2 with 4 that the ability of MDS to discriminate groups of resonances of the same spin is greater in the case of the ^{26}Al data than for ^{30}P. Since the excitation energies and number of decay transitions from resonances are similar

TABLE V. New resonance spins in ^{30}P.

Resonance no.	E_p (MeV)	J^π a	b	c
6	0.957	$1^+,2^+$	2	2
7	1.111	$2^-,3^+$	$2,3^+$	3
13	1.503	$2^-,3^-$	1^+-4^-	≥ 3
16	1.664	$2(1)^+$	1^+-3^-	3
23	1.853	1-4^+	1^+-4^+	1,3
28	2.114	$2^-,3$	3^+	3
33	2.310	$2^-,3^-$	0^+-3^+	2
34	2.369		3^+-5^+	≥ 3
36	2.408		3^+-5^+	≥ 3
37	2.409		3^+	≥ 2
39	2.498	1-3^+	0^+-2^+	1,2
41	2.522	$2(1)^-$	0^+-3^+	1,2
50	3.033		3^+	>2

[a]References [12,13,15].
[b]Decay.
[c]MDS, Fig. 2.

TABLE VI. Lowest 15 bound states of ^{26}Al and ^{30}P populated in the (p,γ) reaction.

^{26}Al E_x (MeV)	J_π	^{30}P E_x (MeV)	J^π
0.0	5^+	0.0	1^+
0.228	0^+	0.677	0^+
0.417	3^+	0.709	1^+
1.058	1^+	1.455	2^+
1.759	2^+	1.974	3^+
1.851	1^+	2.539	3^+
2.069	4^+	2.724	2^+
2.070	2^+	2.840	3^+
2.072	1^+	2.938	2^+
2.365	3^+	3.019	1^+
2.545	3^+	3.734	1^+
2.661	2^+	3.836	2^+
2.740	1^+	3.929	3^+
2.913	2^+	4.144	2^-
3.074	3^+	4.183	2^+

in the two cases, it may be helpful to compare the low-lying structures of the two nuclides. Table VI lists the lowest 15 levels of each nucleus, with spins taken from a recent compilation [15]. These levels receive most of the decay strength of all the resonances considered. It is clear that the dispersion in spins among the low states is somewhat greater in ^{26}Al (0–5) than in ^{30}P (0–3), thus providing more opportunity for different decays for resonances of differing spins. This is likely the single most important determinant of the success of the method. A further difference, also possibly significant, between the data sets is the wider range of spins represented in the resonances of ^{26}Al (1–6) compared to ^{30}P (1–4). Of course, it remains possible that some of the anomalous structure of the maps may arise from incorrect spin assignments in the source data sets, the most likely cause of which would be the existence of unsuspected doublets among the resonances.

Other quantum numbers which affect transition rates, and may therefore affect resonance similarities, are parity and isospin. In the case of ^{26}Al, where full $J^\pi;T$ assignments have been made to most of the resonances studied here and for which the clustering by spin is good, Fig. 4 reveals some discrimination by T for $J=1-4$ and by π for $J=3-5$. It is not surprising that these small effects are not seen in the one-dimensional analysis (Fig. 3), which is dominated by spin selection. In a few cases, it is possible to draw new conclusions regarding parity from Fig. 4.

V. CONCLUSION

The method of multidimensional scaling appears to be a viable means of making simultaneous comparisons of large sets of decay γ-ray spectra from proton capture resonances in order to deduce the spins of the resonances. The utility of the method is greatest where the dispersion in spins of the initial and final states is high. In the case of good spin discrimination, there appears to be some sensitivity to parity and isospin in two-dimensional scaling.

ACKNOWLEDGMENTS

The collaboration of A. M. Al-Soraya, I. A. Al-Agil, and G. U. Din in the ^{30}P measurements is gratefully acknowledged, as are helpful discussions about scaling techniques with C. L. Jones, A. P. M. Coxon, J. B. Kruskal, and F. W. Young. The work was carried out under a grant from the Natural Sciences and Engineering Research Council of Canada.

[1] G. Adams, E. G. Bilpuch, G. E. Mitchell, R. O. Nelson, and C. R. Westerfeldt, J. Phys. G **10**, 1747 (1984).
[2] J. F. Shriner, E. G. Bilpuch, P. M. Endt, and G. E. Mitchell, Z. Phys. A **335**, 393 (1990).
[3] J. Sziklai, J. A. Cameron, and I. M. Szöghy, Phys. Rev. C **30**, 490 (1984).
[4] G. U. Din and J. A. Cameron, Phys. Rev. C **38**, 1164 (1988).
[5] G. U. Din, J. A. Cameron, V. P. Janzen, and R. B. Schubank, Phys. Rev. C **31**, 800 (1985).
[6] P. M. Endt, P. de Wit, C. Alderliesten, and B. H. Wildenthal, Nucl. Phys. **A487**, 221 (1988).
[7] J. A. Cameron, Can. J. Phys. **62**, 115 (1984).
[8] D. G. Kendall, Phil. Trans. R. Soc. London A **269**, 125 (1970).
[9] F. W. Young and R. M. Hamer, *Multidimensional Scaling* (Erlbaum, Hillsdale, NJ, 1987).
[10] G. U. Din and J. A. Cameron, Phys. Rev. C **45**, 2147 (1992).
[11] J. A. Cameron (unpublished).

[12] P. M. Endt, P. De Wit, and C. Alderliesten, Nucl. Phys. **A459**, 61 (1986); **A476**, 333 (1988).
[13] J. P. L. Reinecke, F. B. Waanders, P. Oberholzer, P. J. C. Janse Van Rensburg, J. A. Cilliers, J. J. A. Smit, M. A. Meyer, and P. M. Endt, Nucl. Phys. **A435**, 333 (1985).
[14] S. C. Frankle, G. E. Mitchell, J. F. Shriner, Jr., E. G. Bilpuch, and C. R. Westerfeldt, Phys. Rev. C **45**, 2746 (1992).
[15] P. M. Endt, Nucl. Phys. **A521**, 1 (1990).
[16] E. E. Roskam, MDS(*X*) program series, distributed by Program Library Unit, University of Edinburgh.